Department of Veterans Affairs

Journal of Rehabilitation Research and Development
Vol. 40, No. 1, January/February 2003
Pages 39–48

Kinematic and dynamic performance of prosthetic knee joint using six-bar mechanism

Dewen Jin, Professor; Ruihong Zhang, PhD; HO Dimo, PhD; Rencheng Wang, PhD, Associate Professor; Jichuan Zhang, Professor
Rehabilitation Engineering Center, Department of Precision Instruments, Tsinghua University, Beijing 100084, PR China

Abstract—Six-bar linkages have been used in some prosthetic knees in the past years, but only a few publications have been written on the special functions of the mechanism as used in transfemoral prosthesis. This paper investigates the advantages of the mechanism as used in the prosthetic knee from the kinematic and dynamic points of view. Computer simulation and an experimental method were used in the investigation. The results show that the six-bar mechanism, as compared to the four-bar mechanism, can be designed to better achieve the expected trajectory of the ankle joint in swing phase. Moreover, a six-bar linkage can be designed to have more instant inactive joints than a four-bar linkage, hence making the prosthetic knee more stable in the standing phase. In the dynamic analysis, the location of the moment controller was determined for minimum value of the control moment. A testing prosthetic knee mechanism with optimum designed parameters was manufactured for experiments in the laboratory. The experimental results have verified the advantage revealed in the analyses.

Key words: dynamics, kinematics, prosthetic knee, six-bar mechanism.

INTRODUCTION

Four-bar mechanisms have been widely used in the prosthetic knee for many years and are a subject of investigation by Zarrugh, Radcliffe, Hobson, and other scientists and researchers [1–4]. Six-bar mechanisms have been successfully used in some knee joints, such as Total Knee and 3R60 Knee produced by the Otto Bock Company; a few publications on kinematic and dynamic performance of the six-bar knee mechanism have been reported [5,6]. The general constitution of multiple-bar linkage for the prosthetic knee was outlined by Van de Veen [5], but no further investigations have been reported. Patil and Chakraborty designed a particular six-bar knee-ankle mechanism to provide coordinate motion between knee and ankle joint during walking and squatting [6].

Compared with four-bar mechanisms, six-bar mechanisms have much more design variables. Therefore, with appropriate design, six-bar mechanisms can provide advantages that are more functional. The basic concerns with kinematic and dynamic analyses of a prosthetic knee include the gait pattern (especially the trajectory of ankle joint in swing phase, which provides enough foot ground clearance), angular displacement of the shank, and stability in the standing phase. Moreover, with the intelligent knee developed in the last several years, the desire has been to adapt the prosthesis to walking speed and terrain [7,8]. Therefore, it is necessary to adjust and control the knee moments according to the walking pattern. The values of control moments are the main considerations for developing the moment controller to make it suitable to the prosthetic knee.

In this paper, the kinematic and dynamic performance of the six-bar mechanism used in the prosthetic knee is

Abbreviations: CCD = charge-coupled device, IIJ = instant inactive joint.

This material was based on work supported by the Nature Science Fund No. 39770214 and No. 30170242 of China.

Address all correspondence and requests for reprints to Dewen Jin, Rehabilitation Engineering Center, Department of Precision Instruments, Tsinghua University, Beijing 100084, PR China; tel: 8610-62794189; email: jdw-om@tsinghua.edu.cn.

investigated by computer simulation and some experiments. First, the constitutions of six-bar linkages with total revolute joints are stated. Second, the optimum design procedure is adopted for kinematic design to realize the expected trajectory (spatio-temporal curve) of the ankle joint. Moreover, because more Instant Inactive Joints (IIJs) can exist in six-bar mechanisms than can exist in four-bar mechanisms [9], the stability in the standing phase can be ensured even under some disturbance. For adaptability of the prosthesis to walking speed and terrain, the control moments in the swing phase were investigated in dynamic analysis. The results show that the control moment of the knee joint can be reduced considerably by an appropriate axis being chosen where the moment controller is located. Based on the results of the investigations, a testing prosthetic knee mechanism was manufactured for experimental use in the laboratory. Both analytical and experimental results given in this paper indicate that the advantages of the six-bar linkage can be achieved.

METHODS

Constitution of Six-Bar Mechanisms for Prosthetic Knee

Fundamental types of six-bar mechanisms are the Watt type and Stephenson type as shown in **Figure 1**. Based on these two types, the knee joint has four configurations (see **Figure 2**(**a**) to (**c**)). The design parameters of these configurations are the same. The particular objective is to constitute the six-bar knee mechanism so that the shank is fixed to link 5 or 6 while the thigh is fixed to link 1. Otherwise, for example, if the shank is connected to link 3, then the function of the six-bar knee mechanism will be the same as that of four-bar mechanisms.

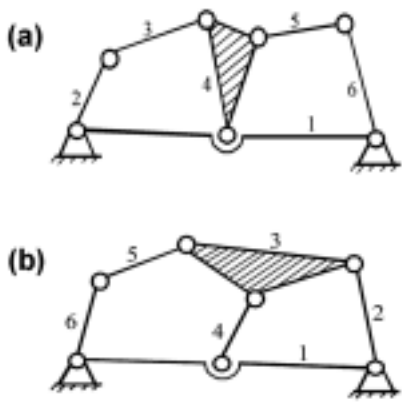

Figure 1.
Basic six-bar mechanism: **(a)** Watt type and **(b)** Stephenson type.

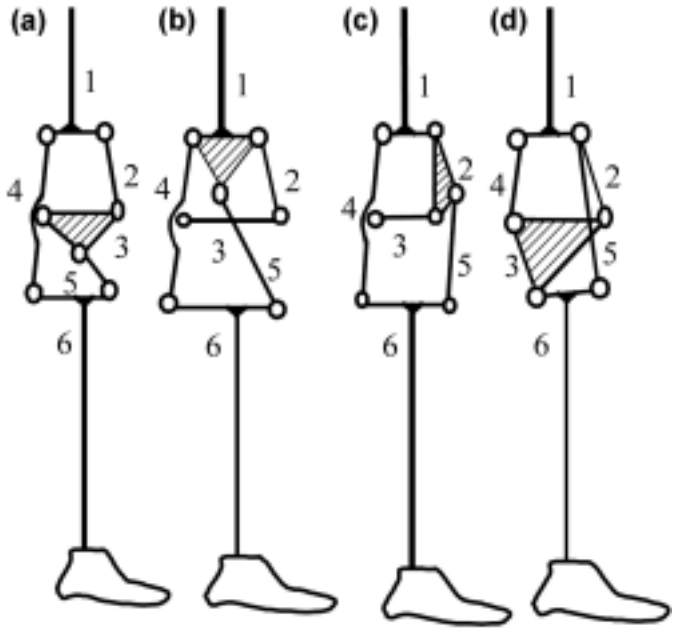

Figure 2.
Configurations (**a**) 1, (**b**) 2, (**c**) 3, and (**d**) 4 of six-bar mechanism for prosthetic knee.

Kinematic Design of Six-Bar Mechanism

The kinematic design aims to achieve the expected trajectory of the ankle joint and the locus of the geometric center of the knee mechanism and to ensure the stability in the extended position of the knee. Meanwhile, the dimensions of links should be within an acceptable range. The geometric center of the knee mechanism can be calculated by the equations

$$x_{gc} = \frac{1}{7}\sum_{i=1}^{7} x_i$$

$$y_{gc} = \frac{1}{7}\sum_{i=1}^{7} y_i \quad ,$$

where x_{gc}, y_{gc} are the coordinates of the geometric center of the knee mechanism and x_i, y_i are the coordinates of the seven joints of the mechanism.

To meet the requirements just mentioned, we adopted the optimum procedure. The optimization is based on the expected relative motion of thigh and shank. As an example, taking the configurations shown in **Figure 2**(**a**) with

the shank and link 5 connected (**Figure 3**), the optimization problem is expressed in the subsequent paragraphs.

Objective Function

$$F(X) = C_1 \sum_{i=1}^{n} \sqrt{\left|\tilde{x}_{Pi} - x_{Pi}\right|^2 + \left|\tilde{y}_{Pi} - y_{Pi}\right|^2} + C_2 \sum_{i=1}^{n} \sqrt{\left|\tilde{x}_{Ki} - x_{Ki}\right|^2 + \left|\tilde{y}_{Ki} - y_{Ki}\right|^2} \quad (1)$$

$$\min_{x \in R^{16}} F(X) = \min_{x \in R^{16}} \left[C_1 \sum_{i=1}^{n} \sqrt{\left|\tilde{x}_{Pi} - x_{Pi}\right|^2 + \left|\tilde{y}_{Pi} - y_{Pi}\right|^2} + C_2 \sum_{i=1}^{n} \sqrt{\left|\tilde{x}_{Ki} - x_{Ki}\right|^2 + \left|\tilde{y}_{Ki} - y_{Ki}\right|^2} \right],$$

where n is the number of selected points in a gait cycle, $n = 25$; x_{Pi}, y_{Pi} are the calculated coordinates of the trajectory of the ankle joint during the optimum process; $\tilde{x}_{Pi}, \tilde{y}_{Pi}$ are the coordinates of the expected trajectory of the ankle joint; x_{Ki}, y_{Ki} are the calculated coordinates of the trajectory of the geometrical center of the knee joint during the optimum process; $\tilde{x}_{Ki}, \tilde{y}_{Ki}$ are the coordinates of the expected trajectory of the knee joint; and C_1,C_2 are the weight factors and $C_1 + C_2 = 0.9 + 0.1 = 1$. C_1 is much larger than C_2 here, because emphasis is put on the locus of the ankle joint.

How to choose the expected trajectory is a problem needed to make further studies. What we used here is based on the gait analysis of the sound side of a transfemoral prosthesis user while walking at a normal speed (1.2 m/s), because we hope to increase the level of symmetry of gait parameters.

Design Parameters

By defining a frame xOy fixed on the thigh, shown in **Figure 3**, the design parameters can be expressed as a vector **X** such that

$$\mathbf{X} = [x_1, x_2, ..., x_{16}]^T = [l_1, l_2, l_3, ..., l_{14}, \theta, \beta]^T. \quad (2)$$

The variables in the vector are as indicated in **Figure 3**. There are, in total, 16 elements, including 14 dimensions of links and two angular positions of the thigh and shank θ and β, respectively. The coordinates of the points *A, B, C, D, E, F, G, I, J*, and *P* in the frame are expressed as functions of the design parameters in the following equations:

$$x_A = x_I - l_{11} \sin\theta \quad (3)$$

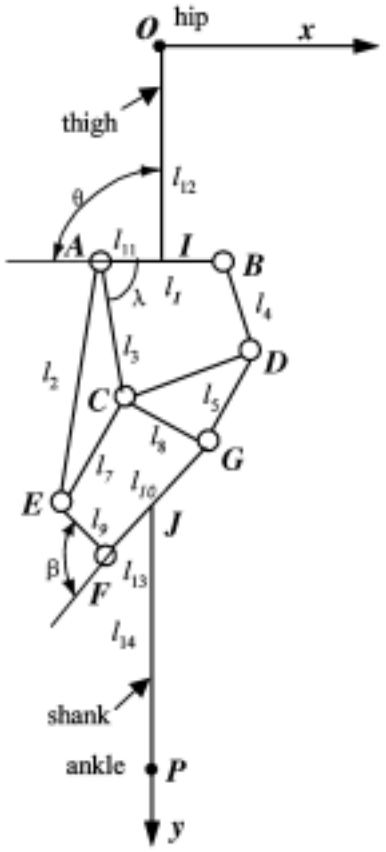

Figure 3.
Design parameters for optimization.

$$y_A = y_I + l_{11} \cos\theta \quad (4)$$

$$x_B = x_I + (l_1 - l_{11}) \sin\theta \quad (5)$$

$$y_B = y_I - (l_1 - l_{11}) \cos\theta \quad (6)$$

$$(x_C, y_C) = \mathrm{Fun}xy(x_A, y_A, x_B, y_B, \lambda, l_3) \quad (7)$$

$$(x_D, y_D) = \mathrm{Fun}xy(x_C, y_C, x_B, y_B, \cos^{-1}\left(\frac{\sqrt{l_5^2 + l_1^2 + l_3^2 - l_4^2 - 2l_1 l_3 \cos\lambda}}{2l_5\sqrt{l_1^2 + l_3^2 - 2l_1 l_3 \cos\lambda}}\right), l_5) \quad (8)$$

$$(x_E, y_E) = \mathrm{Fun}xy(x_A, y_A, x_C, y_C, \cos^{-1}\left(\frac{\sqrt{l_2^2 + l_3^2 - l_1^2}}{2l_2 l_3}\right), l_2) \quad (9)$$

$$(x_G, y_G) = \mathrm{Fun}xy(x_C, y_C, x_D, y_D, \cos^{-1}\left(\frac{\sqrt{l_5^2 + l_8^2 - l_6^2}}{2l_5 l_8}\right), l_8) \quad (10)$$

$$(x_F, y_F) = \mathrm{Fun}xy(x_E, y_E, x_G, y_G, \cos^{-1}\left(\frac{\sqrt{(l_9^2 - l_{10}^2 + (x_E - x_G)^2 + (y_E - y_G)^2}}{2l_9\sqrt{(x_E - x_G)^2 + (y_E - y_G)^2}}\right), l_9) \quad (11)$$

$$x_J = x_F + \frac{l_{13}}{l_{10}}(x_G - y_F) \quad (12)$$

$$y_J = y_F + \frac{l_{13}}{l_{10}}(y_G - y_F) \quad (13)$$

$$x_P = x_J - l_{14}\cos(\tan^{-1}\frac{y_G - y_F}{x_G - x_F} + \beta) \quad (14)$$

$$y_P = y_J - l_{14}\sin(\tan^{-1}\frac{y_G - y_F}{x_G - x_F} + \beta)\ , \quad (15)$$

where "Fun*xy*" is defined in Equation (16) as

$$\mathrm{Fun}xy(x_1, y_1, x_2, y_2, \xi, l)\begin{cases} x = x_1 + \dfrac{(x_2 - x_1)\cos\xi + (y_2 - y_1)\sin\xi}{\sqrt{((x_2 - x_1)^2 + (y_2 - y_1)^2)}}l \\ y = y_1 + \dfrac{(x_1 - x_2)\sin\xi + (y_2 - y_1)\cos\xi}{\sqrt{((x_2 - x_1)^2 + (y_2 - y_1)^2)}}l \end{cases}, \quad (16)$$

where l is the distance between points R and S and ξ is the angle between the two lines S-R and T-R. Equation (16) is used to calculate the coordinates of an arbitrary point $R(x,y)$ based on coordinates of the other two known points $S(x_1, y_1)$ and $T(x_2, y_2)$.

Constraints

Self-locking condition in the extended knee position is given by

$$\frac{y_E - y_F}{x_E - x_F} = \pm \frac{y_F - y_G}{x_F - x_G}, \qquad (17)$$

when

$$\frac{y_I - y_H}{x_I - x_H} = \frac{y_P - y_J}{x_P - x_J}.$$

Dimensional limitation of links is

$$l_{i\min} < l_i \le l_{i\max} \qquad (i = 1, 2, ...14), \qquad (18)$$

where l_i is the same as defined in Equation (2) and $l_{i\min}$ and $l_{i\max}$ are the dimension limitation to the length of each bar.

Displacement bounds of the mechanism are

$$(x_A, x_B, x_C, x_D, x_E, x_F, x_G)_{\max} - (x_A, x_B, x_C, x_D, x_E, x_F, x_G)_{\min} \le X_{\max} \qquad (19)$$

$$(y_A, y_B, y_C, y_D, y_E, y_F, y_G)_{\max} - (y_A, y_B, y_C, y_D, y_E, y_F, y_G)_{\min} \le Y_{\max}, \qquad (20)$$

where the limited values of the design variables $l_{\min}$, $l_{\max}$, $X_{\min}$, and $Y_{\min}$ were given based on the required size of the mechanism.

RESULTS AND DISCUSSION

After the optimization method of Complex Penalty Function is applied, the design parameters are obtained as

$$\mathbf{X} = [x_1, x_2, ..., x_{16}]^T = [l_1, l_2, l_3 ... l_{14}, \theta, \beta]^T$$
$$= 25, 71.6, 40, 37.9, 28, 21.8, 31.7, 19, 17,$$
$$35, 32, 383, 14, 267, 88°, 11°]^T.$$

Then the six-bar knee mechanism was designed, and the trajectory generated by the mechanism can be obtained by the kinematic analysis being appied.

The comparison of the generated trajectory of the ankle joint with expected ones is shown in **Figure 4**. The mean square errors for ankle and knee are $\mathrm{Err}_{\mathrm{ankle}} = 1.96\%$ and $\mathrm{Err}_{\mathrm{knee}} = 11.43\%$, respectively. The comparison of the trajectory of the ankle joint in swing phase of the six-bar linkage knee with that of a four-bar knee mechanism is also made and given in **Figure 5**. The dimensions of the four-bar linkage were designed with the use of the same procedure as that used for the six-bar linkage knee. The mean square error of ankle joint trajectories of the four-bar mechanism is 6.71 percent, while that of the six-bar mechanism is 1.96 percent.

Moreover, when the user is walking on different terrain, such as on a slope or in different speeds, the six-bar knee mechanism possesses advantages from the kinematic point of view. The comparison is shown in **Figure 6(a)** to **(c)**, and the mean square errors are listed in the **Table**.

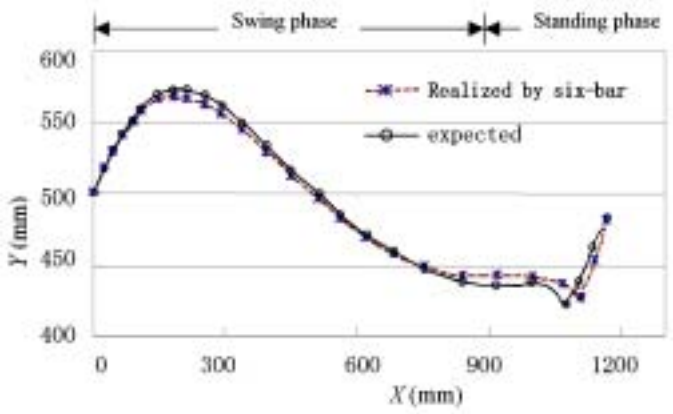

Figure 4.
Trajectory of ankle joint by optimal six-bar linkage.

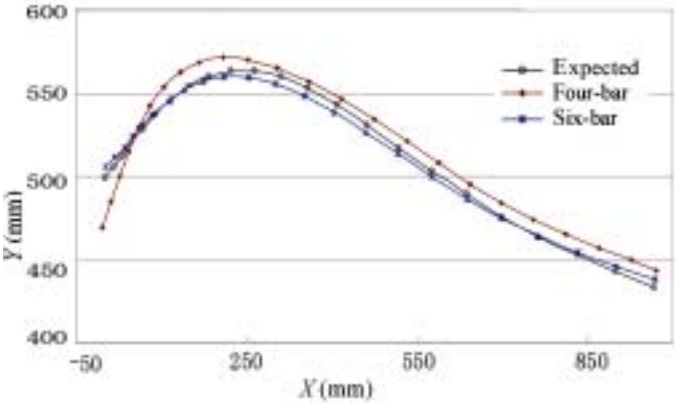

Figure 5.
Comparison of ankle joint trajectory in swing phase between different mechanisms.

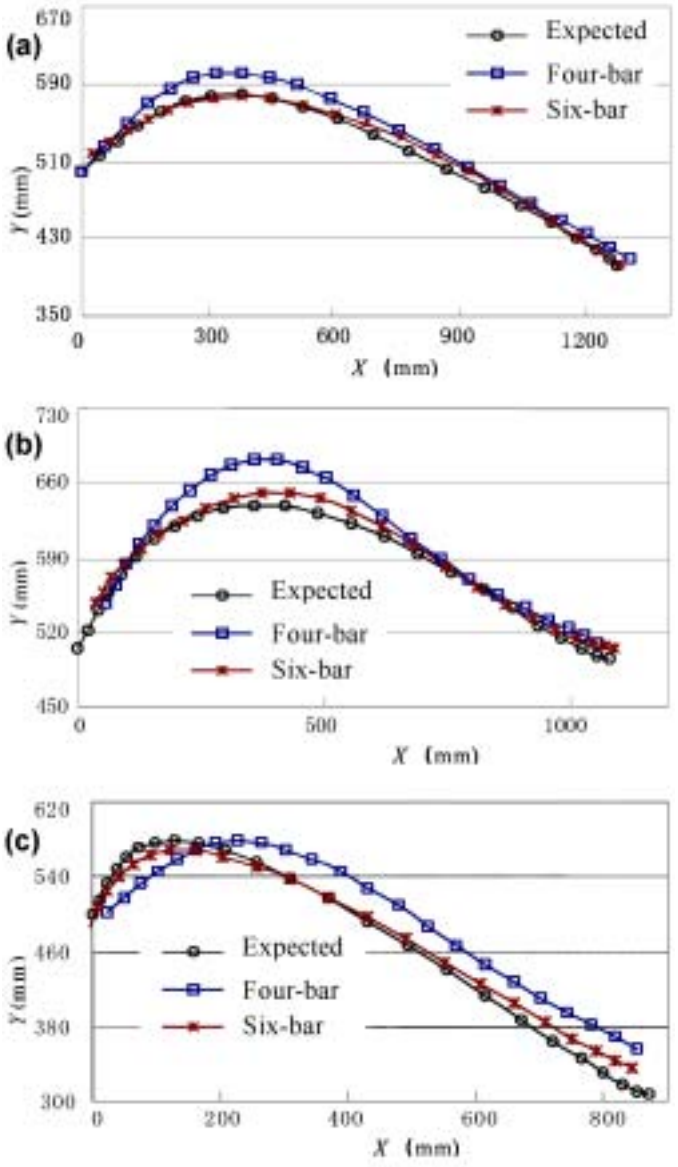

Figure 6.
Trajectory of ankle joint in swing phase in different walking pattern: **(a)** fast walking, **(b)** up hill, and **(c)** down hill.

Table.
Mean square errors of ankle joint trajectories in different patterns (%).

Walking Pattern	Four-Bar	Six-Bar
Fast	5.16	2.27
Slow	6.71	1.96
Up Slope	9.87	3.97
Down Slope	11.9	4.61

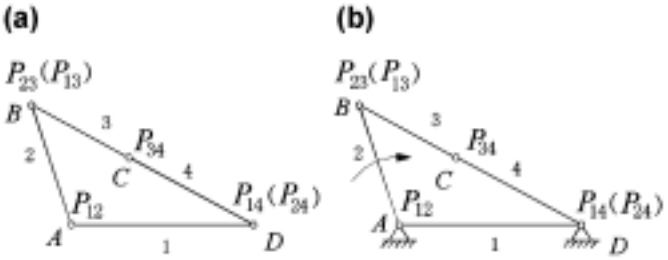

Figure 7.
Instant inactive joint of four-bar mechanism (*P* is instant velocity center; subscripts represent the number of bars): (**a**) four-bar kinematic chain and (**b**) four-bar mechanism with link 1 fixed.

Instant Inactive Joints in Six-Bar Mechanism and Stability Design of Prosthetic Knee Joint

In the multibar kinematic chain, if two links connected by a revolute joint have the same angular velocity in this position (or at this instant time), which means that no relative motion exits between these two links, the joint is referred to as IIJ. For example, if the four-bar kinematic chain, shown in **Figure 7(a)**, is in such a position that links 3 and 4 are collinear and links 1 and 2 have the same angular velocity, then the revolute joint *A* is an IIJ in this position. The IIJ must exist for the mechanism to be self-locking. In **Figure 7(b)**, if link 1 (or 2) is fixed, link 2 (or 1) cannot drive the mechanism no matter how large the driving moment is. Obviously, the more IIJ exists, the more stable the mechanism is. In the four-bar kinematic chain, only one IIJ can exist. However, in the six-bar kinematic chain, as many as four IIJs exits, depending on the design. For example, when links 2 and 3 of the six-bar kinematic chain are collinear as shown in **Figure 8**, the P_{14}, P_{16}, P_{45}, and P_{56} joints will be IIJs. Therefore, when link 1 is fixed, the mechanism will be stable despite any disturbance applied on links 4, 5, or 6. In the optimum design stated in the last section, the constraint (equation 17) means links *EF* and *FG* (**Figure 3**) are collinear in the extended position of the knee. In this case, the *A*, *B*, *C*, and *D* joints are IIJs. Therefore, in addition to the functional advantage in kinematic design mentioned in the last section, the six-bar linkage for the prosthetic knee has another advantage based on stability.

Dynamic Analysis and Knee Moment Control in Swing Phase

Kinematic design is based on the expected relative motion between thigh and shank. To realize the expected absolute motion of the shank and corresponding ankle joint trajectory requires not only kinematics but also dynamic analysis and control. One could obtain the expression for

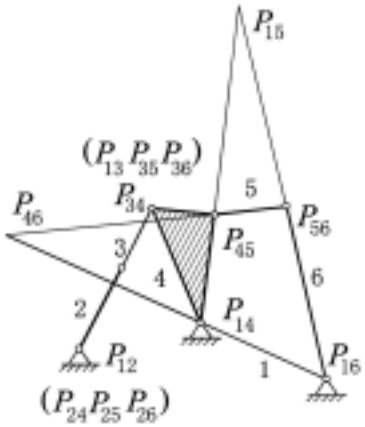

Figure 8.
Instant inactive joint of six-bar linkage (*P* indicates the instant velocity center; subscripts represent the number of bars).

the control moment by using the inverse dynamic procedure. The control moment is usually applied on the knee joint. Essentially, the small control moment will be easier to be realized than large ones.

To determine the suitable axis where the control moment is to be applied, we performed the dynamic analysis for the mechanism to derive the control moment. **Figure 9** depicts the free body diagrams for dynamic force analysis. To demonstrate the dynamic process, taking axis *A* (**Figure 3**) as an example (i.e., the control moment is supposed to be applied on joint *A)* and considering the balance of the moments and forces for each body (**Figure 9)**, the procedure to determine the moment can be obtained by

$$F_{fe}=\frac{-F_{xd}\overrightarrow{GT_y}+F_{yd}\overrightarrow{GT_x}-(m_sg+m_sa_{sy})\overrightarrow{GS_x}+(m_sa_{sx})\overrightarrow{GS_y}-J_s\ddot{\theta}_s}{d_{G-\overrightarrow{FE}}} \quad (21)$$

$$\begin{cases} G_x= -F_{fe}\cos\theta_{xfe}+m_sa_{sx}-F_{xd} \\ G_y= -F_{fe}\sin\theta_{xfe}+m_sg+m_sa_{sy}-F_{yd} \end{cases} \quad (22)$$

$$F_{db}=\frac{-G_x\overrightarrow{CG_y}+G_y\overrightarrow{CG_x}}{d_{C-\overrightarrow{DB}}}, \quad (23)$$

where $\overrightarrow{GT}_x$, $\overrightarrow{GT}_y$, denote the distances between *G* and *T* in *x,y* directions, respectively; $\overrightarrow{GS}_x$, $\overrightarrow{GS}_y$, denote the distances between *G* and *S* in *x,y* directions, respectively; m_s, J_s are the mass and the moment of inertia of the shank and foot respectively; a_{sx}, a_{sy} and $\ddot{\theta}_s$ represent the acceleration of the mass center *S* in *x,y* directions and angular acceleration of the leg, respectively. They were obtained from the expected movement of the shank. $d_{G-\overrightarrow{EF}}$ is the perpendicular distance from point *G* to line *EF* and similarly to other points and lines, and $\theta_{xfe}, \theta_{xdb}, F_{fe}, F_{db}, G_x, G_y$, and M_A are indicated in **Figure 9**. Finally, the control moment M_A is derived from the equation

$$M_A= -F_{ef}\,d_{A-\overrightarrow{EF}}-F_{db}d_{A-\overrightarrow{DB}}+G_x\overrightarrow{AG_y}-G_y\overrightarrow{AG_x}. \quad (24)$$

By applying the same procedure, the control moments M_B, M_G, and M_F can be determined, too. The calculated results of M_A and M_B, M_G, and M_F in normal walking speed are plotted in **Figures 10** and **11,** respectively. The values in the vertical axis are the moments divided by the weight of the body *W*. One can observe that the values of M_A are extremely larger than those of M_B, M_G , and M_F, whereas M_F is the smallest. Therefore, selecting axis *F* as the place where the control moment should be applied would be most appropriate.

Considering that the control moments depend on walking speed and terrain, such as going up or down hill, analyzing them in different walking situations is necessary. The moments required at axis *F* in the swing phase in different walking situations are shown in **Figure 12**.

In a practical prosthetic knee, usually the total control moment consists of two parts: the positive extension moment, acting to extend knee provided by an extension assist spring, and the negative resistance moment, produced by a damper. The control moment shown in **Figure 12** is the total knee moment. To derive the moment of the damper that is controllable, one must minus the spring toque from the total moment. The resulting moment provided by the controllable damper is shown in **Figure 13**.

Experiments

Based on the analysis just mentioned, a prosthetic knee mechanism was manufactured for experimental use (**Figure 14**). It consists of a six-bar linkage, a friction damping moment generator whose moment can be controlled by computer through a step motor (see Dewen Jin et al. for details [8]).

In the experiments, the prosthetic thigh was strapped to the thigh of a nonamputee subject to make the thigh move as close as possible to normal gait. It was dragged along in normal walking speed. The movement of the shank and the trajectory of ankle joint were recorded with a CCD (charge-coupled device) based human motion detecting and analysis system, which was developed at Tsinghua University [10]. The block diagram is shown in **Figure 15**.

The effectiveness of the analyses and design presented in this paper was evaluated with the use of the mean square error of the trajectory of the ankle joint E_{ra}

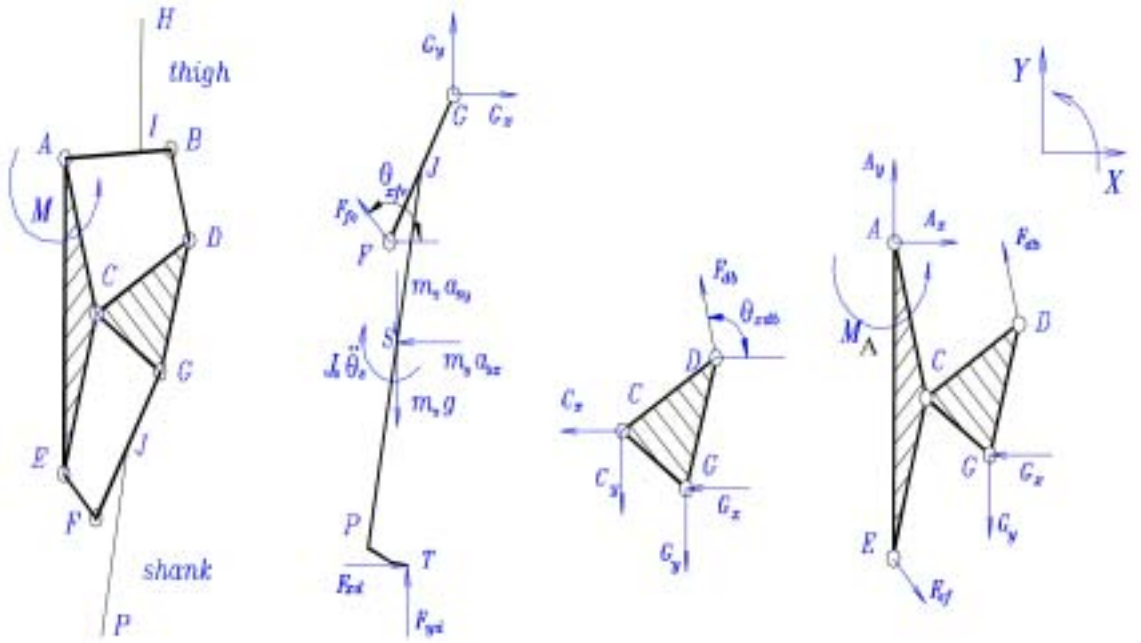

Figure 9.
Free body diagram of six-bar mechanism when torque applied on joint *A*.

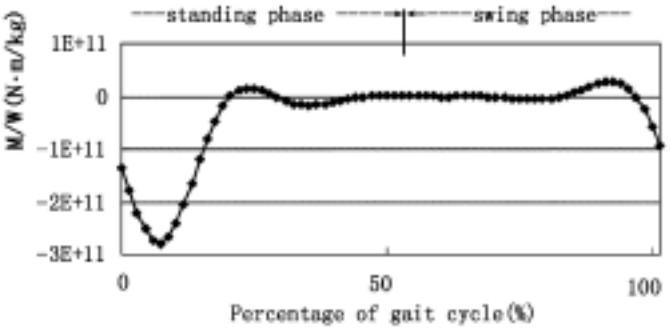

Figure 10.
Control moment M_A.

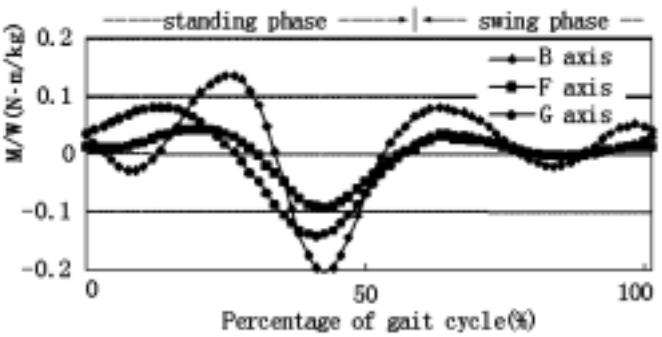

Figure 11.
Control moments M_B, M_G, and M_F.

(mean square errors = up slope 5.97%, down slope 5.73%, level [fast] 5.67%, and level [slowly] 4.06%) and the angular displacement of shank E_{rs} (up slope 5.40%, down slope 4.17%, level [fast] 4.39%, level [slowly] 2.46%), by

$$E_{ra} = \frac{\sqrt{|\tilde{x}-x|^2 + |\tilde{y}-y|^2}}{\sqrt{|\tilde{x}-\tilde{x}(1)|^2 + |\tilde{y}-\tilde{y}(1)|^2}}$$

and

$$E_{rs} = \frac{\sqrt{\sum(\theta_k - \tilde{\theta}_k)^2}}{\sqrt{\sum \tilde{\theta}_k^2}},$$

where x,y and θ_k are experimental values, $\tilde{x}, \tilde{y}$ and $\tilde{\theta}_k$ are expected values, and $\tilde{x}(1)$, $\tilde{y}(1)$ are reference values.

CONCLUSIONS AND DISCUSSION

The six-bar prosthetic knee mechanism has been investigated from kinematic and dynamic points of view in this paper. The performance of the knee mechanism is shown in the following aspects:

- The trajectory of the ankle joint and the movement of the shank can be much closer to that expected than to that of the four-bar linkage if one were to

apply the optimum design procedure proposed in this paper.

- The values of control moments in swing phase were found to vary in a very large range when taking different axes as the place where the controller is located. The dynamic analysis is important for determining the most suitable place for knee moment control.
- Since more IIJs exist in a six-bar linkage than in a four-bar linkage, a six-bar is more capable of maintaining stability in standing phase under interference.

The knee mechanism was developed experimentally to show the feasibility of the procedures used in the investigation. To develop it for clinical application, further development (such as the reduction of the size and weight of the step motor, development of a smaller electric circuit with battery, the use of light and high strength material, etc.), should be undertaken. Furthermore, determining what is the most appropriate expected trajectory that can increase the level of symmetry of gait pattern remains an interesting and systematic subject. It has been found that the gait parameters of the sound side of a transfemoral prosthesis user are also affected by the prosthesis side. The factors which affect the gait pattern include not only the kinematic and dynamic performance of the prosthetic knee but also the construction of the ankle joint, functions of prosthetic foot, the quality of alignment, and the physical

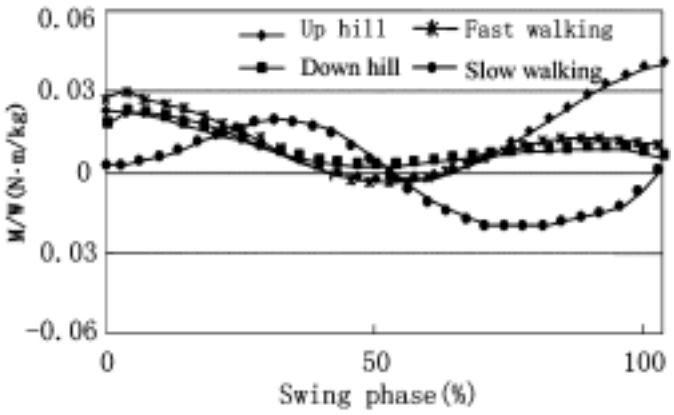

Figure 12.
Total moments needed on *F* axis.

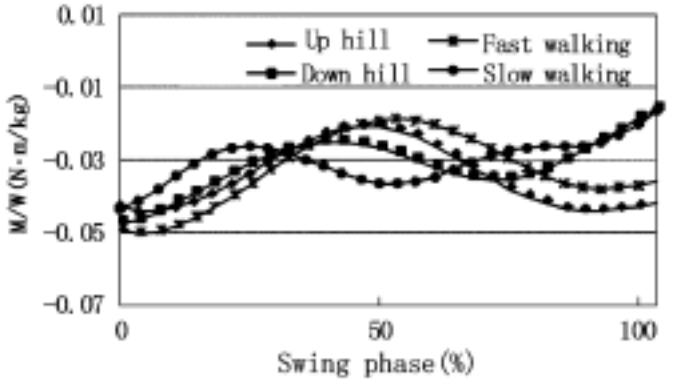

Figure 13.
Moments provided by controllable damper.

Figure 14.
Six-bar mechanism knee for experiment.

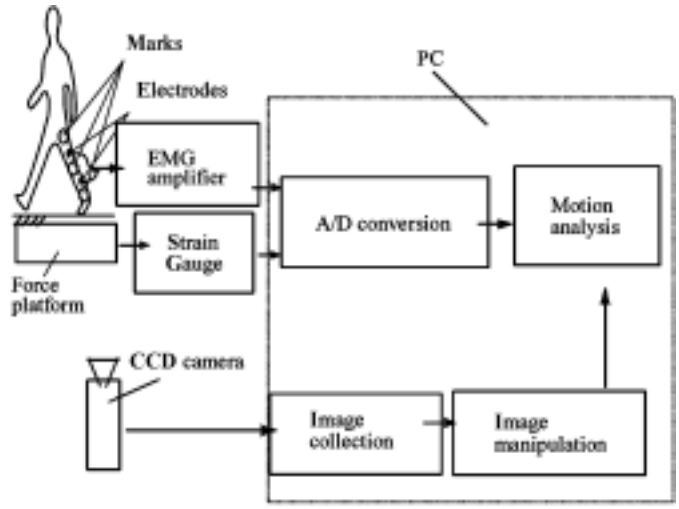

Figure 15.
Block diagram of gait analysis system.

and psychological conditions of the user. Therefore, to obtain the most appropriate expected trajectory, further studies and clinic tests are needed. This paper focuses on the kinematic and dynamic design of the six-bar prosthetic knee mechanism. Certainly, the proper design of the prosthetic knee mechanism will be helpful to improve the level of symmetry of gait pattern.

REFERENCES

1. Zarrugh MY, Radcliffe CW. Simulation of swing phase dynamics in above-knee prostheses. J Biomech 1996;9(5): 283–92.
2. Hobson DA, Torfason LE. Computer optimization of polycentric prosthetic knee mechanisms. Bull Prosthet Res 1975;(10–23):187–201.
3. Hobson DA, Torfason LE. Optimization of four-bar knee mechanism—a computerized approach. J Biomech 1974; 7(4):371–76.
4. Radcliffe CW. Four-bar linkage prosthetic knee mechanisms: kinematics, alignment and prescription criteria. Prosthet Orthet Int 1994;18:159–73.
5. Van de Veen PG. Principles of multiple-bar linkage mechanisms for prosthetics knee joints. Abstract of the 8th World Congress, ISPO; 1994 Apr 2–7; Melbourne, Australia. p. 55.
6. Patil KM, Chakraborty JK. Analysis of a new polycentric above-knee prosthesis with a pneumatic swing phase control. J Biomech 1991;24(3,4):223–33.
7. Nakagawa A. Intelligent knee mechanism and the possibility to apply the principle to other joint. Proceedings of the Annual International Conference of the IEEE Engineering in Medicine and Biology; 1998 Oct. 29–Nov 1; Hong Kong, China. p. 2282–87.
8. Dewen Jin, Ruihong Zhang, Jichuan Zhang, Rencheng Wang, William A. Gruver. An intelligent above knee prosthesis with EMG based terrain identification. Proceedings of 2000 IEEE International Conference on System, Man and Cybernetics; 2000; Nashville, Tennessee. p. 1859–64.
9. Ruihong Zhang, Dewen Jin, Jichuan Zhang, Analysis of the temporal inactive joints in multi-linkage mechanisms. J Tsinghua Univ Sci Technol 2000;40(4):39–42.
10. Wang Rencheng, Huang Changhua, Wang Jijun, Bai Caiqing, Yang Niangfeng, Jin Dewen. Human motion analysis system based on common video-camera. J Biomed Eng 1999;16(4):448–52.

Submitted for publication July 3, 2001. Accepted in revised form May 3, 2002.